Dynamics of concentration fluctuations in a heterocoordinated binary liquid alloy

M. Soltwisch and D. Quitmann
Institut für Atom- und Festkörperphysik, Freie Universität Berlin, D-1000 Berlin 33, Germany

H. Ruppersberg and J. B. Suck*
Institut Laue-Langevin, Boîte Postale 156X, F-38042 Grenoble, France
(Received 25 February 1983)

The quasielastic part of the scattering law has been measured for the concentration fluctuations, $S_{cc}(q,E)$, of a binary liquid with compound-forming tendency, $Li_{0.80}Pb_{0.20}$. In this neutron scattering experiment on a time-of-flight (TOF) spectrometer (resolution 0.28 meV), a range of momentum transfers q of $0.27 < q < 2.5$ Å^{-1} was studied which includes the prominent first peak of $S_{cc}(q)$; the energy range studied varies from $-1 \cdots +1$ to $0 \cdots +16$ meV, with increasing q values. The sample was measured at 1.04, 1.13. and $1.20T_{melt}$. From the TOF spectra, the self-diffusion constant of ^{7}Li and the interdiffusion constant for $Li_{0.80}Pb_{0.20}$ were extracted. The latter, which reveals a pronounced narrowing of the quasielastic width around the peak of $S_{cc}(q)$, can be interpreted to yield a lifetime of Li-Pb agglomerates. An extension of a relation which connects self- and interdiffusion constants is discussed. A simple description of elastic, i.e., $E=0$, scattering is achieved. Good fits to the data are obtained using a Mori description; although the LO mode is not seen in the spectra, some hint as to its characteristic frequency can be derived. The fits require a sum of two relaxation terms for which the widths and relative strength are obtained as functions of q. The fast mechanism may contain an indication for coupling of concentration fluctuations to conduction electrons.

I. INTRODUCTION

In binary liquid alloys the relative arrangement of the *A* and *B* atoms reflects the prevailing mechanism of interaction between these particles, and it is a basic ingredient for a description of the properties of such systems. Compilations of thermodynamic data, e.g., by Komarek,[1] indicate that ideal behavior of binary liquid alloys is rather exceptional, i.e., in quite a few systems the *A* and *B* particles are not distributed at random, see, e.g., Ref. 2. In fact, diffraction data of a large number of systems indicate domination of *A-A* and *B-B* nearest-neighbor pairs (preferred self-coordination) or of *A-B* nearest neighbors (preferred heterocoordination) in systems which from thermodynamics are known to have a tendency for segregation or compound formation, respectively. A recent review is given by Chieux and Ruppersberg.[3] A number of models and theories has been proposed to describe this chemical short-range order (CSRO) and to relate it to various other properties.

However, very little experimental data exist for what may be called the lifetime of the preferred atomic arrangements in heterocoordinated alloys. For such a system, liquid $Li_{0.8}Pb_{0.2}$, we present here quasielastic neutron scattering data which yield—to our knowledge for the first time—experimental information about the dynamics of concentration fluctuations on a microscopic scale.

Such information is expected to be of interest for a discussion of models of transport coefficients, of crystallization or glass formation, or for the explanation of quadrupolar nuclear-spin-relaxation rates.[4] The experimental investigation of the dynamics is also an indispensable test for liquid-state models which often differ considerably near $E=0$, or for the potentials used in their simulation (see, e.g., Ref. 5). Considerable theoretical effort has already been devoted to molecular dynamics of binary liquids, e.g., Refs. 6–9, to predictions of the spectral shape and the moments, Refs. 10(a) and 10(b), and to analytical treatments (see Refs. 11 and 12 for recent reviews).

It has been mentioned above that information about CSRO is obtained from diffraction experiments. In general, however, it is quite impossible to extract from a single measured scattering intensity directly that portion which is modulated by CSRO. Only for very few special alloys[3] is CSRO scattering observed directly by neutron diffraction. One of these so-called "zero alloys" is $^7Li_{0.80}Pb_{0.20}$ (or $^7Li_4Pb$, for short), which must be prepared from the enriched isotope ^{7}Li and from natural lead. A strong preference for unlike nearest neighbors has been observed in solid[13] as well as in liquid[14,15] $Li_{1-c}Pb_c$ alloys. The composition dependences of all known properties deviate strongly from an ideal behavior, with maximum deviations close to $c_{Pb}=0.2$, which also corresponds closely to the composition of the intermetallic compound with the highest melting point of the system. The anomalous behavior and the CSRO are probably due to a transfer of charge from the Li to the Pb sites which renders the bonding partially ionic.[16,17] According to Ruppersberg and Egger[14] and Ruppersberg and Reiter,[15] the global atomic arrangement in liquid Li-Pb is similar to that of a monatomic melt with superimposed CSRO which is especially pronounced and long ranged close to the composition Li_4Pb.

Bhatia and Singh[18] as well as Hoshino and Young[19]

were able to calculate thermodynamic properties using the concept of distinct complexes of Li_4Pb. An alternative to this "chemical" or "molecular" point of view is the concept of concentration fluctuations introduced by Bhatia and Thornton[20] which has proven to be very powerful; it is in these terms that we shall work for the most part of the present paper, and the connection to the molecular viewpoint will also be established explicitly.

A zero-scattering alloy has been investigated earlier by neutron inelastic scattering.[21] In that case, however, the study was made to investigate self-diffusion in $Cu_{0.525}Ni_{0.475}$ from the incoherent scattering, and the zero alloy was chosen only to reduce the disturbing coherent scattering, which is the main subject here.

After introducing scattering laws in Sec. II, the experiment will be described in Sec. III, and the data presented in Sec. IV. The discussion in Sec. V will first consider diffusional dynamics, then the $E=0$ (elastic) scattering and the concept of molecular lifetime will be considered; its main part is devoted to a Mori description of $S_{cc}(q,E)$. Section VI contains some concluding remarks. Parts of the results of the present work have been published earlier.[22–24]

II. SCATTERING LAWS

From the experimental data we are able to calculate $I^a(q,E)$ which is the scattered intensity per atom, given in barn units (10^{-24} cm^2) as a function of momentum transfer q (Å^{-1}) and energy transfer E (meV). This intensity consists of a coherent and an incoherent part,

$$I^a(q,E)=I^c(q,E)+I^i(q,E) , \tag{1}$$

which will be discussed separately.

In the case of the $^7Li_{0.8}Pb_{0.2}$ alloy under investigation, the coherent part is proportional to $S_{cc}(q,E)$ which is one of the three number-concentration partial structure factors, S_{NN}, S_{Nc}, and S_{cc}, introduced by Bhatia and Thornton to describe the scattering laws related to number-density and concentration fluctuations in binary systems,[20]

$$\sigma S(q,E)=4\pi[\langle b\rangle^2 S_{NN}(q,E)+2\langle b\rangle(\Delta b)S_{Nc}(q,E) +(\Delta b)^2 S_{cc}(q,E)] , \tag{2a}$$

where $\sigma=4\pi\langle b^2\rangle$. In our case where $\langle b\rangle=0$,

$$I^c(q,E)=4\pi(\Delta b)^2 S_{cc}(q,E) . \tag{2b}$$

$\Delta b=b_A-b_B$ is the difference between the coherent scattering lengths of the two species and b is related to the coherent scattering cross section by $\sigma^{\rm coh}=4\pi b^2$. The average scattering length $\langle b\rangle=c_A b_A+c_B b_B=0$ for $^7Li_{0.80}Pb_{0.20}$, and thus $S_{NN}(q,E)$ and $S_{Nc}(q,E)$ do not contribute to $I^c(q,E)$. $S_{cc}(q,E)$ is the scattering law for the neutrons to exchange energy E with concentration fluctuations of wave number q. The zeroth-frequency moment is the corresponding static structure factor,

$$S_{cc}(q)=\int_{-\infty}^{\infty} S_{cc}(q,E)dE . \tag{3}$$

For large q, $S_{cc}(q)$ approaches $c_A c_B$, and $I^c(q,E)$ approaches

$$c_A\sigma_A^{\rm coh}S_{sA}(q,E)+c_B\sigma_B^{\rm coh}S_{sB}(q,E) .$$

The above-mentioned preference for heterocoordination of Li_4Pb in r space may directly be deduced from a sine transform of the complete $S_{cc}(q)$ curve.

The long-wavelength limit $S_{cc}(0)$ is proportional to the mean-square concentration fluctuations and it becomes related to thermodynamic data via the curvature of the free energy G in the G-c diagram, i.e., the stability $\partial^2 G/\partial c^2$,

$$S_{cc}(0)=N\langle(\Delta c)^2\rangle=Nk_B T\left[\left[\frac{\partial^2 G}{\partial c^2}\right]_{p,T}\right]^{-1} . \tag{4}$$

In the framework of the conformal-solution model we have, for $q=0$,

$$S_{cc}(0)=\frac{S_{cc}^{id}(0)}{1+2W(0)S_{cc}^{id}(0)/k_B T} , \tag{5a}$$

where $W(0)$ is related to the enthalpy of mixing ΔH,

$$W(0)=\Delta H/(Nc_A c_B) , \tag{5b}$$

and $S_{cc}^{id}(q=0)=c_A c_B$. Since this identity holds for all q, an extension of Eq. (5a) for finite q values is possible by introducing a q-dependent effective potential $W(q)$.[25]

Dynamic structure factors of binary liquids for small q and E have been derived by Cohen, Sutherland, and Deutch[10(a)] and formulated for $S_{cc}(q,E)$ by Bhatia, Thornton, and March.[10(b)] In the hydrodynamic limit the overdamped diffusional motion of concentration fluctuations leads to a Lorentzian line shape of the $S_{cc}(q,E)$-vs-E curve

$$S_{cc}(q,E)=S_{cc}(0)\frac{\Gamma^+/2\pi}{E^2+(\Gamma^+/2)^2} \quad \text{for } q\to 0,\ E\to 0 . \tag{6a}$$

The full width at half maximum (FWHM) Γ^+ defines the interdiffusion constant D^+ by the usual relation

$$\Gamma^+=2\hbar q^2 D^+ . \tag{6b}$$

A second Lorentzian term derived in Refs. 10(a) and 10(b) is essentially determined by heat conduction. Since liquid $Li_{0.80}Pb_{0.20}$ has electronic and thus high heat conductivity, we neglect the second Lorentzian in comparison to Eq. (6). A more general form for $S_{cc}(q,E)$ will be introduced in Sec. V C.

The macroscopic interdiffusion or chemical-diffusion constant D^+ is connected in approximation to the self-diffusion constants D_A, D_B for the constituent atoms in the same system via Darken's relation[26] (see also Ref. 27),

$$D^+=\bar{D}c_A c_B/S_{cc}(0) , \tag{7a}$$

with

$$\bar{D}=c_A D_B+c_B D_A . \tag{7b}$$

Incoherent scattering from lead is very weak so that only lithium contributes to the $I^i(q,E)$ term in Eq. (1),

$$I^i(q,E)=c_{\rm Li}\sigma_{\rm Li}^{\rm inc}S_{s\rm Li}(q,E) . \tag{8}$$

$\sigma_{\rm Li}^{\rm inc}$ is the incoherent cross section. We will assume that

for the scattering law an equation analogous to (6) holds for all q,E,

$$S_{s\mathrm{Li}}(q,E)=\frac{1}{\pi}\frac{\hbar q^2 D_{\mathrm{Li}}}{E^2+(\hbar q^2 D_{\mathrm{Li}})^2} . \quad (9)$$

III. EXPERIMENT

Starting from 99.999%-pure Pb and Li enriched to more than 99%-pure ^{7}Li (bought from Oak Ridge National Laboratory), $^7Li_{0.80}Pb_{0.20}$ was prepared in a dry box filled with continuously recycled high-purity argon. The correct composition of the sample was controlled by chemical analysis. The sample was filled into cylindrical Ta cans of 15 mm i.d. and 100 mm height. In the irradiated area the wall thickness was 0.1 mm. The cans were sealed by electron-beam welding.

The neutron scattering experiment was performed at the time-of-flight (TOF) spectrometer IN5 of the Institut Max von Laue—Paul Langevin in Grenoble. The sample was placed in a cylindrical furnace 500 mm in diam. The heater consisted of two Mo cylinders with a foil thickness of 50 μm each. They were surrounded by two Ti radiation shields, each 50 μm thick.

The temperature was measured with a W-Re thermocouple positioned in a dead hole in the can's top. Runs were made at nominally 1023, 1098, and 1173 K. We suppose that the temperature of the sample corresponds to these values ± 2 K. Stability during the measurement was ± 2 K.

The neutron beam was collimated outside the vacuum vessel by boron-loaded plastic to a height of 46 mm and to a width just exceeding the sample diameter. The correct positioning was checked by the shadow image on a film. In order to achieve sufficient energy resolution of the quasielastic scattering and to include the first $S_{cc}(q,E)$ peak, an energy of the incident neutrons of $E_0=4.09$ meV was chosen corresponding to $\lambda_0=4.47$ Å. A total of 400 ^{3}He detectors were grouped in 84 banks positioned at 42 different scattering angles between 8.2° and 124°; thus two independent TOF spectra per angle were obtained. The range of q covered was 0.2—2.5 Å^{-1} (for zero-energy transfer), so that coherent elastic Ta or Mo reflections were avoided. The four choppers were set to produce neutron pulses 100 μs wide and 10 ms apart. Each TOF spectrum was collected in 512 channels, each 18 μs wide.

For calibrations and corrections, additional measurements were made for the following arrangements. (1) Furnace without sample at 1023 K. (2) A vanadium sheet wound spirally to the same dimensions as the sample. (3) A cylindrical Cd sheet resembling the sample. (4) The Cd sheet in the empty can. (The last three all at room temperature.) (5) An empty Ta can at 1073 K. These control data were collected before the Li_4Pb runs; furnace, vanadium, and the empty can were repeated in the end. Actual measuring times for Li_4Pb were about 40 h per temperature. The neutron-beam intensity was monitored by two thin, flat boron counters placed in front of and behind the vacuum vessel. After inspection of the spectra from the 84 banks, ten banks had to be rejected because of high background or background changes during the course of the experiment. For the other 32 angles the two spectra were added together.

IV. DATA EVALUATION

A. Normalization, background, self-shielding, and absorption

All spectra were divided by the integral intensity of the monitor in front of the furnace, and by the corresponding integral elastic vanadium intensities, the intensity of the vanadium spectra having been corrected by the Debye-Waller factor. The energy dependence of the detector sensitivity was also corrected.

The correction for background was performed by subtracting the empty can run from the Li_4Pb runs, and the furnace run from the vanadium spectra. The difference between the two background spectra was negligibly small, indicating that the scattering from the Ta container was very weak. The small elastic peaks (integral intensities $\simeq 0.2$ b) could be identified as scattering from the monitor beyond the vacuum vessel and from the vessel itself. In the subtraction of the empty can runs actually the transmission factors of the Li_4Pb [$T_S(E_0)=0.77$] and of the vanadium sample [$T_v(E_0)=0.76$] must be applied, to account for the self-absorption of incident and scattered neutrons in the samples. However, from the background spectra including the Cd run, it was decided to subtract the background with no shielding factor at all ($T=1$). The error introduced thereby is within the statistical noise.

From the measured transmission $T_s=0.77$ one obtains for the cylindrical sample a linear shielding coefficient $\mu_s=0.227$ cm^{-1} which in turn gives a total cross section per atom $\sigma_{\mathrm{total}}=\mu_s A_s/\rho_s N_L=5.69$ b ($\rho_s=3.11$ g/cm^3, $A_s=47$ g/mole, and $N_L=$Avogadro's number). This is much larger than the scattering cross section

$$c_{\mathrm{Li}}\sigma_{\mathrm{Li}}^{\mathrm{inc}}+c_{\mathrm{Pb}}c_{\mathrm{Li}}4\pi(\Delta b)^2=3.4 \quad (10)$$

(measured in b), where cross sections from the literature have been used for Pb and ^{7}Li (see Table I). The additional reduction of the transmitted beam was ascribed to ^{6}Li, of which 0.1% will produce the effect. The spectra were then corrected for self-shielding using the well-known formula for a cylindrical sample. In correcting for self-shielding by scattering and absorption inside the sample, the absorption of ^{7}Li and of Pb is negligible because the cross sections are small.

TABLE I. Cross sections and scattering lengths used.

	b (fm)	σ^{inc} (b)	σ^{abs} (b)
Natural Pb	+0.94		
^{7}Li	−0.229	0.80	
^{6}Li			2360[a]
V		5.1	11.6[a]

[a]At $\lambda=4.47$ Å.

B. Conversion to (q,E) spectra, detailed balance

The TOF spectra were converted from the (θ,t) grid of the measurement to a (θ,E) grid (with θ equal to the scattering angle) by taking the $E=0$ time from the peak position of vanadium spectra and calculating the neutron energy change for each time channel. Using a five-point spline function, we then interpolated between the different (θ,E) spectra at each of the selected q values to obtain the (q,E) spectrum. The q values were chosen as $q=4\pi\lambda^{-1}\sin(\theta/2)$, i.e., each (q,E) spectrum coincides with a measured (θ,E) spectrum at $E=0$. Finally, the symmetrized scattering law was calculated by multiplying with $\exp(E/2k_BT)$. The density of points per (q,E) area obtained in this way was chosen approximately equal to the local density of original experimental points.

C. Reduction to absolute cross sections

With the use of the known cross section of vanadium (Table I) the vanadium measurement enables one to reduce the Li_4Pb spectra to absolute cross sections. The V sample was a rolled cylinder of the same dimension as the Li_4Pb sample; its mean density was calculated from the transmission ($T_v=0.76$, $\mu_v=0.233$ cm^{-1}, and $\rho_v=1.18$ g/cm^3 corresponding to a packing fraction of 20%). Knowing the size and density of the Li_4Pb probe, we obtain the scattering intensity in barns which at this stage will be called $I^{\text{meas}}(q,E)$.

D. Correction for multiple scattering

From an estimate using the method of Blech and Averbach[28] which works well for energy-integrated multiple scattering (MSC) in the case of incoherent scattering, one gets for $^7Li_{0.8}Pb_{0.2}$ with the cross sections listed in Table I and the ratio, tube radius/tube height equal to 0.163, a MSC cross section of $\sigma_m=0.35$ b. Since this is about 10% of the single scattering cross section and may introduce sizable errors, especially at low scattering angle where the intensity is mainly determined by the incoherent ^{7}Li scattering (0.64 b per scattering unit $Li_{0.8}Pb_{0.2}$), a more accurate correction was needed.

MSC was calculated using Copley's computer program.[29] This program simulates the actual scattering process measured by a TOF spectrometer. The main input data are the following: the ideal scattering law, the scattering geometry, the distribution in energy and time of the incident neutrons, and the absorption and scattering cross sections. The ideal scattering law was constructed from the experimental spectra $I^{\text{meas}}(q,E)$. We have assumed that MSC results predominantly from the main peak in the structure factor where the relative influence of multiple processes themselves is small. The spectra $I^{\text{meas}}(q,E)$ are a convolution of the scattering intensity with the resolution profile $V(E)$,

$$I^{\text{meas}}(q,E)=I^{a}(q,E)\otimes V(E)+I^{M\text{ex}}(q,E)\otimes V(E)\ . \quad (11)$$

$I^{M\text{ex}}(q,E)$ is the experimental MSC before resolution broadening. $V(E)$ has been obtained from the vanadium spectra, which were nearly triangular in shape (FWHM=0.28 meV) and could well be fitted by a sum of three Lorentzians; the energy dependence of the resolution was neglected. For $I^{a}(q,E)+I^{M\text{ex}}(q,E)$ we used again a sum of three Lorentzians because the convolution of Lorentzians can be performed analytically. A fit of the right-hand side (rhs) of Eq. (11) to the experimental $I^{\text{meas}}(q,E)$ yielded the six parameters for $I^{a}+I^{M\text{ex}}$ at each q. Since the MSC correction calculated thus, $I^{M\text{calc}}$, was an overestimate, we had to reduce it by a factor of 0.85. In all analyses we have neglected the possibility of a cusp or very narrow line at $E=0$.

An uncertainty introduced by using the measured spectra as input for the MSC calculations is the necessity of extrapolating the scattering law used into regions actually not measured. For $q<0.5$ Å^{-1} the measured energy range is less than 3 meV, increasing to about 20 meV at $q=2.5$ Å^{-1}; for higher q values one does not measure the $E=0$ part of the spectrum. We have extrapolated out to $q=9$ Å^{-1} the areas (nearly constant) and the widths (slowly increasing) of the three Lorentzians constituting $I^{a}+I^{M\text{ex}}$. The energy extrapolation up to 20 meV at low q was simply performed by using the fitted Lorentzians in that range.

MSC spectra were computed at every second detector for 35 TOF channels covering the energy range -3 to $+16$ meV. The program used 1500 neutrons which gave sufficient statistics. The MSC intensity integrated from -3 to $+16$ meV amounted to about 0.3 b, nearly independent of the scattering angle [see Fig. 2(b) of Ref. 22]. This compares well with the value 0.35 b calculated according to Blech and Averbach. The MSC spectra (smoothed and interpolated) were subtracted from the measured spectra before the self-shielding correction and the results were then corrected for self-shielding. The resulting fully corrected experimental spectra are called

$$I^{\text{expt}}(q,E)=I^{\text{meas}}(q,E)-0.85I^{M\text{calc}}(q,E)\ .$$

The importance of the MSC correction is strongest in the wings of the quasielastic spectra. There the intensity is often reduced by up to 30% which has a pronounced effect on the second-moment evaluation. The MSC spectra are included in Fig. 3. There is a slight asymmetry near $E=0$ the reason of which is unknown. For the higher temperatures, MSC is slightly broader in energy, while the energy-integrated value remains the same within 10%.

E. Results

In Fig. 1 a perspective representation of $I^{\text{expt}}(q,E)$ is given for the three temperatures. Part of the data appears in detail in Figs. 2 and 3 for some selected q values and $E<3$ meV; the energy range $E=0$–16 meV is presented in Fig. 4. Data for $E>16$ meV are not presented since the MSC correction was calculated only for $E<16$ meV. Also the experimental results for $q>2.57$ Å^{-1} are omitted since $I^{\text{meas}}(q,0)$ was not obtained in the present experiment beyond that q value. It may be useful to state, however, that a very smooth monotonous decay of the intensity was observed outside the 16-meV limit in each of the spectra.

The energy integral of the scattering law is extended at most to 16 meV,

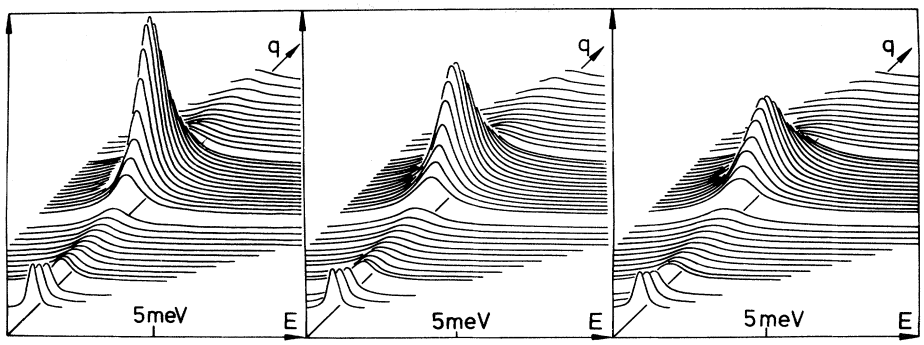

FIG. 1. Symmetrized experimental scattering laws $I^{expt}(q,E)$ for liquid $^7Li_{0.80}Pb_{0.20}$. Temperatures are 1023, 1098, and 1173 K (from left to right). Structure peak occurs at $q_0 = 1.50$ Å^{-1}.

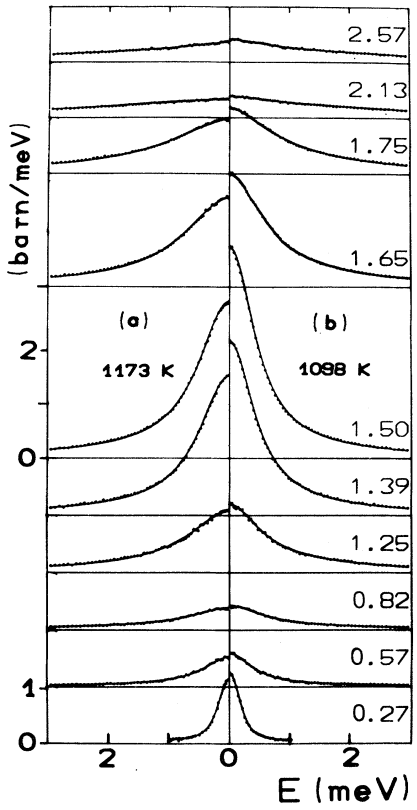

FIG. 2. Scattering intensity for liquid $^7Li_4Pb$ at ten momentum transfers ($q = 0.27$–2.57 Å^{-1}) for the quasielastic region at 1173 K (curves *a*) and 1098 K (curves *b*). Circles are experimental data for $I^{expt}(q,E)$ with the corrections described in Secs. IV A–IV D. Solid lines are spectra $I^a(q,E) \otimes V(E)$, i.e., including resolution broadening, from the Mori fit. For each temperature, only the energy-gain side is shown.

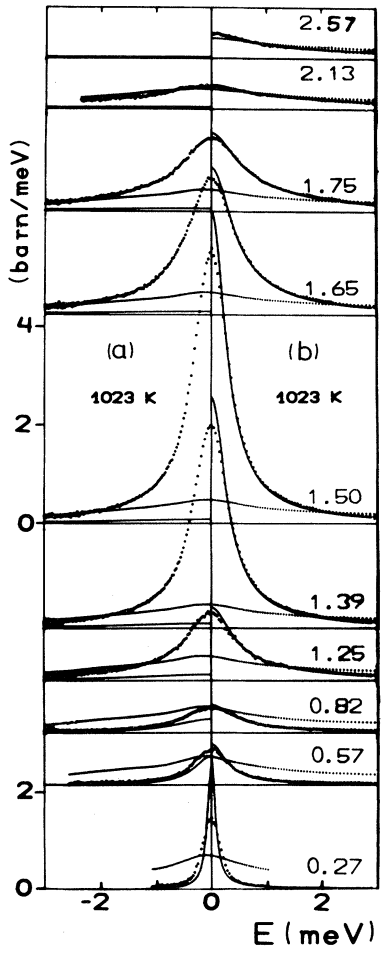

FIG. 3. As in Fig. 2, scattering intensity $I^{expt}(q,E)$ at 1023 K is presented by circles; the energy-gain (b) and -loss sides are shown. Dotted line is 10 times the MSC correction applied, $8.5I^{Mcalc}(q,E)$, the factor of 10 being added for easier recognition. Solid curve is on the rhs of the fit spectrum $I^a(q,E)$; on the energy-loss side, the solid curve shows the incoherent Li contribution $I^i(q,E)$ only. Resolution broadening effect can easily be seen near $E = 0$.

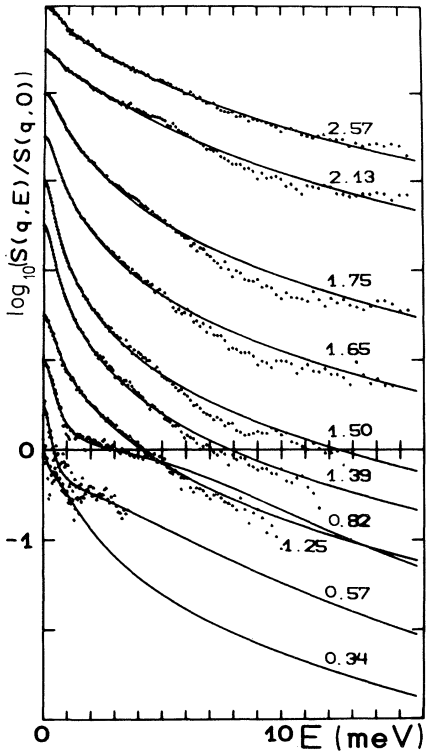

FIG. 4. Logarithmic spectrum shapes at ten momentum transfers for 1023 K, normalized to the $E=0$ value: $S_{cc}(q,E)/S_{cc}(q,0)$. Fit curves are from the Mori fits with $E_{vib}=60$ meV. Curves for $q=0.57$–2.57 Å^{-1} have been shifted upward by factors of $10^{0.5}$. Note the change in shape between the third and fourth curve from below (0.8 and 1.25 Å^{-1}); at larger q, the data may suggest a "plateau and step" between 3 and 8 meV.

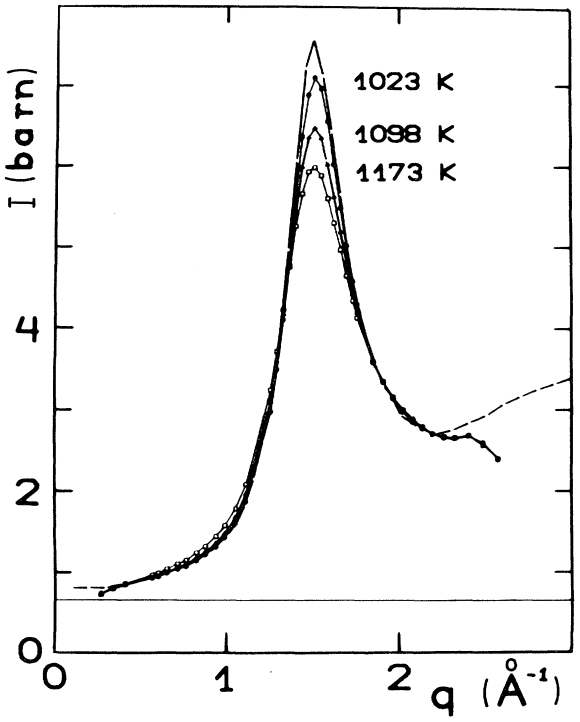

FIG. 5. Static structure factor $I^{expt}(q)$ of liquid $^7Li_{0.80}Pb_{0.20}$ as defined in Eq. (12). Dashed line: result of Ref. 15 interpolated for 1023 K from 995 and 1075 K. Horizontal line marks $c_{Li}\sigma_{Li}^{inc}$. As $q\to 0$, the concentration-fluctuation structure factor $4\pi(\Delta b)^2 S_{cc}(q)$ approaches (2.75 b)(0.054) for 1023 K (see Ref. 24). Fit results for $S_{cc}(q)$ exceed the values from Eq. (12) by at most 5% for all q, except for the one low point at $q=0.27$ and the last five points, where the fits follow the dashed curve.

$$I^{expt}(q)=\int_{E_{min}}^{|E_{min}|} I^{expt}(q,E)dE + 2\int_{|E_{min}|}^{E_{max}} I^{expt}(q,E)dE \ . \quad (12)$$

$E_{max}(q)$ is the maximum energy transfer covered or 16 meV, whichever is smaller, correspondingly E_{min} is $E_{min}(q)$ or -3 meV, whichever is more positive. $I^{expt}(q)$ is presented in Fig. 5 including $I^i(q)=0.65$ b.

Besides the MSC correction, the largest sources of *systematic* uncertainty are presumably the conversion from the (θ,t) grid to the (q,E) grid, including the necessary interpolations, and the subtraction of $I^i(q,E)$ to be discussed in Sec. V A 1.

The dynamic structure factor at zero-energy transfer, i.e., the elastic scattering $S_{cc}(q,E=0)$, is presented in Fig. 6.

We note here that some of the q dependences show unexpected "fine structure" which is correlated in the three temperatures (e.g., $\bar{D}$ in Fig. 12 at and beyond 1.8 Å^{-1}). These are very likely systematic errors of normalization. The reduced experimental spectra can be obtained on magnetic media (floppy disk or tape) from one of the authors (Soltwisch).

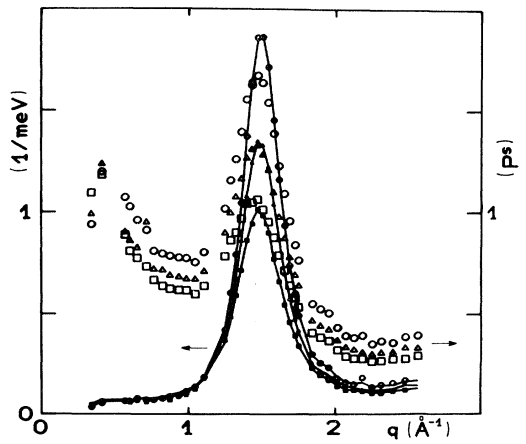

FIG. 6. Elastic concentration-fluctuation structure factor, $S_{cc}(q,0)/c_{Li}c_{Pb}$, for liquid Li_4Pb is shown as connected points, left-hand scale, for 1023 (top curve), 1098, and 1173 K. Unconnected points are lifetimes of concentration fluctuations with wave vector q, $\tau_{cc}(q)$ as defined by Eq. (18), right-hand scale applies.

V. ANALYSIS AND DISCUSSION

A. Diffusion approximation

1. Li self-diffusion and Li-Pb interdiffusion

At $q<0.5$ Å^{-1}, $S_{cc}(q)$ and thus $I^c(q)$ is very small and the incoherent scattering from ^{7}Li dominates the scattered intensity. This is a fortunate circumstance in so far as it allows the determination of the self-diffusion constant of Li, $D_{\rm Li}$ from Eq. (9) with little ambiguity.

Since $D_{\rm Li}$ is obtained from incoherent neutron scattering, it corresponds to the tracer-diffusion constant. For the results see Table II. Errors are estimated to be about $\pm 10\%$. These diffusion constants are lower by about a factor of 1.5 than the extrapolation of the pure Li metal value[30] to the present temperatures; the apparent activation energy (between 1023 and 1173 K) is about 7 kcal/mole, much higher than in pure Li.

Inserting $D_{\rm Li}$ from Table II into Eq. (9) yields $S_{s{\rm Li}}(q,E)$ from which $I^i(q,E)$ is calculated using Eq. (8). Combining Eqs. (1) and (2) finally yields $S_{cc}(q,E)$. Since the incoherent Li spectrum is considerably broader than the $S_{cc}(q,E)$ spectrum, the ensuing uncertainty of the resulting $S_{cc}(q,E)$ was considered tolerable at $q>0.5$ Å^{-1}.

In principle, the interdiffusion constant D^+ should be obtained from $S_{cc}(q\to 0, E\to 0)$ by applying the diffusional ansatz, Eq. (6). For $q<0.5$, however, as has been mentioned above, $I^c(q)$ becomes very small as compared with $I^i(q)$, and it was not possible to obtain the $S_{cc}(0,E)$ values. In addition, Eq. (6) does not take LO modes into account which might exist in liquid Li_4Pb, as shown in Sec. V C 1 of this paper.

However, the shape of the experimental data suggests the application of an extension for finite q of Eq. (6), which is obtained by substituting $S_{cc}(q)$ for $S_{cc}(0)$ on the rhs of this equation. Values of $D^+(q)$ obtained in this way have been published earlier,[22–24] and in Table II, values are given for $q_1=1.25$ Å^{-1} where $S_{cc}(q)=c_Ac_B$, and for $q_0=1.5$ Å^{-1}, which corresponds to the peak of $S_{cc}(q)$ (see lines 5 and 6). The observed narrowing of $S_{cc}(q,E)$ around q_0 is just a demonstration of the de Gennes narrowing expected at q_0.[10(b)] However, it appears noteworthy that this narrowing of the peak near $E=0$ derived theoretically from the second frequency moment of the dynamic structure factor is as well developed in the case of $S_{cc}(q,E)$ as it is for $S_{NN}(q,E)=S(q,E)$ in simple liquids. A discussion of $S_{cc}(q,E)$ in terms of two Lorentzians has been given in Refs. 22 and 23. The diffusion ansatz for $S_{cc}(q,E)$ suggests three additional viewpoints to which we turn to in Secs. V A 2, V A 3, and V B.

2. Extension of Darken's relation

As a phenomenological extension of the concept of interdiffusion to finite q, we generalize $S_{cc}(0)$ of Eq. (5a) to $S_{cc}(q,E)$ by first using the conformal solution ansatz, Eq. (5a), generalized to finite q [$W(0)$ and $S_{cc}(0)$ replaced by $W(q)$ and $S_{cc}(q)$, respectively]; secondly, we replace $S_{cc}^{id}(q)=c_Ac_B$ in Eq. (5a) by the hydrodynamic ansatz for $S_{cc}(q,E)$,

TABLE II. Diffusion constants (10^{-5} cm^2/s) in liquid $^7Li_{0.80}Pb_{0.20}$.

		1023 K	1098 K	1173 K
1	$D_{\rm Li}$[a]	17.5	21.3	27.4
2	$D_{\rm Pb}$[b]	2.9	3.3	3.5
3	$\bar{D}$ (q_0)[c]	5.8	6.9	8.2
4	D^+ (q_0)[d]	2.4	3.2	4.2
5	D^+ (q_1)[e,f]	5.9	6.8	7.7
6	D^+ (q_0)[e]	2.3	3.0	3.9

[a]Fit at $q=0.20$ Å^{-1}, assuming two Lorentzians, viz., $S_{s{\rm Li}}(q,E)$ and $S_{cc}(q,E)$.
[b]From $\bar{D}$ line 3, $D_{\rm Li}$, and Eq. (7b).
[c]From Mori fit and Eq. (28).
[d]From $\bar{D}$ line 3 using Eq. (15).
[e]From fitting two Lorentzians, $S_{s{\rm Li}}(q,E)$ and $S_{cc}(q,E)$.
[f]At $q_1=1.25$ Å^{-1}, we have $S_{cc}(q_1)=c_{\rm Li}c_{\rm Pb}$, thus $D^+=\bar{D}$.

$$S_{cc}^{id}(q,E)=S_{cc}^{id}(q)\frac{\bar{\Gamma}/2\pi}{E^2+\bar{\Gamma}^2/4}\ . \tag{13}$$

$W(q)$ is then determined from the known zeroth moment $S_{cc}(q)$,

$$W(q)=-\frac{k_BT\pi\bar{\Gamma}}{4c_Ac_B}\left[1-\left[\frac{c_Ac_B}{S_{cc}(q)}\right]^2\right]\ . \tag{14}$$

Rearranging the resulting expression for $S_{cc}(q,E)$, one arrives again at a Lorentzian shape, which, however, has now a width $\Gamma^+(q)=2\hbar q^2D^+(q)$ with

$$D^+(q)=\bar{D}\frac{c_Ac_B}{S_{cc}(q)}\ . \tag{15}$$

The effective-field approximation taken over from a description of the structure thus introduced the effect of structure into the dynamics, exactly in the same way as given by Darken's relation, Eq. (7a) (Ref. 26), of which Eq. (15) may be considered as an extension to finite q. Certainly this result is only a rough approximation, notwithstanding its possible usefulness for practical purposes. A more precise approximation is Eq. (28). We note here that a simple Lorentzian representation of $S_{cc}(q,E)$ roughly reproduces the observed spectra. However, there are systematic deviations at all q values. A relation of the Eq. (15) type has long been in use for density fluctuations in simple fluids where it connects the coherent, collective width with the single-particle width and the structure factor: Sköld derived it for Ar as $\Gamma=2\hbar q^2D_s/S(q)$ or

$$S(q,E)=S(q)S_s(q/\sqrt{S(q)},E)$$

using other arguments.[31]

Accepting Eq. (15) as correct, $D^+(q)$ leads to estimates for $\bar{D}$ (see line 5 of Table II). From Eq. (7b) and $\bar{D}$ one can derive $D_{\rm Pb}$ also (see Table II). $D_{\rm Pb}$ is not very precise (in particular, it depends strongly on $\bar{D}$, the value of which depends on q), but it is smaller than an extrapolation of the pure liquid-Pb values[32] to the present temperatures.

That the ratio of diffusion constants of the heavy and light component does not need to agree with the simple scaling $D_{\rm Pb}/D_{\rm Li}\simeq\sqrt{m_{\rm Li}/m_{\rm Pb}}=0.18$ derived from

thermal velocities only, has been discussed for LiBr by Lantelme *et al.*[33]

3. $S_{cc}(q,E=0)$: *Elastic scattering*

As was mentioned in the Introduction, some processes such as spin relaxation or solidification occur on a time scale which is slow compared to the diffusional (or other) motion of the concentration fluctuations. The decisive quantity for these processes is thus $S_{cc}(q,0)$. For this kind of application we must look first of all for a simple analytical representation of $S_{cc}(q,E\simeq 0)$. Adopting the mean-field ansatz just described which works very well for $E=0$ with an (nearly q-independent, T-dependent) average diffusion constant $\bar{D}$, one has

$$S_{cc}(q,0)\simeq \frac{S_{cc}(q)^2}{c_A c_B}\frac{1}{\pi\hbar q^2\bar{D}} . \tag{16}$$

For the data see Fig. 6. Note the steep rise on either side of $q=q_0$, caused by the combined action of $S_{cc}(q)^2$ and $1/q^2$. The temperature dependence is extremely large, a fact which is best accentuated by noting that a plot of the inverse of the peak height of $S_{cc}(q_0,0)$ vs T cuts zero only 10% below the melting point.

B. Concentration fluctuations and formation of molecules

It has been mentioned in the Introduction that liquid Li_4Pb displays strong spatial correlations between the deviations of Li or Pb concentrations from the average. This fact as well as the anomalous behavior of other properties has been related to the existence of Li_4Pb molecules by several authors (see Refs. 18, 19, and 34).

The molecular models consider an equilibrium between a local structure, agglomerate, or molecule and its dissociated constituents, treating this mixture as a ternary or pseudobinary system. The equilibrium concentration of the ordered phase, i.e., of the agglomerate, is to first order (i.e., neglecting entropy changes) determined by the interaction energy $W(q)$ of Eq. (5). This average concentration appears in the present experiment in the static structure factor $S_{cc}(q)$: The deviation of $S_{cc}(q)$ from $c_A c_B$ is proportional to the number of molecules; for $q=0$, see Eq. (A3) of Ref. 35.

The average concentration is in fact the result of a dynamical equilibrium, and the present paper is concerned with the *rate* at which the spatial concentration-fluctuation waves decay. The Lorentzian form for the dynamics which we have assumed so far implies an exponential time decay of the agglomerates as in the simplest version of a chemical rate equation.

For the purpose of discussion, it will be useful to give a more precise meaning to the term "lifetime of the agglomerate" which we shall call τ_{cc}: Starting from the time-dependent form of the concentration-concentration correlation, viz., the intermediate scattering function

$$I_{cc}(q,t)=\frac{1}{\hbar}\int_{-\infty}^{\infty} S_{cc}(q,E)e^{iEt/\hbar}dE , \tag{17}$$

the lifetime of a concentration fluctuation with wave vector q is

$$\tau_{cc}=\int_{-\infty}^{\infty} I_{cc}(q,t)dt/2I_{cc}(q,0)$$

or

$$\tau_{cc}(q)=\pi\hbar\frac{S_{cc}(q,0)}{S_{cc}(q)} . \tag{18}$$

These times are included in Fig. 6. They show a smooth increase toward small q values, and superimposed on it a peak at q_0. This maximum of τ_{cc} indicates that the concentration fluctuation with wave vector q_0, and with them the above-mentioned agglomerates, have an increased lifetime.[36]

The approximations used so far yield, for Eq. (18),

$$\tau_{cc}(q)\simeq\frac{1}{q^2D^+}\simeq\frac{1}{q^2\bar{D}}\frac{S_{cc}(q)}{c_A c_B} . \tag{19}$$

We interpret Eq. (19) in the sense that there are two dynamical processes involved: an average transport by diffusion leading to $1/\bar{D}q^2$ (in chemical rate language it may represent the need to remove or supply reactants) and $S_{cc}(q)/c_A c_B$ as a retardation due to binding of the agglomerate (thus the analog of the usual exponential factor containing the activation energy for formation of the structure). The temperature dependence of $\tau_{cc}(q)$ is dominated in the present case by $\bar{D}$.

A qualifying remark must be added: While a discussion of dynamics in terms of a reaction, molecule $\leftrightarrow$ constituents, is illustrative, the long range of the concentration correlations and the first-shell coordination numbers suggest that a realistic model must be more complicated, including collective ordering; see the recent analysis of Ruppersberg and Reiter.[15] In the scattering experiment information is obtained about the correlation of one or two particles. These are not two "tagged" particles (as, e.g., in dipolar broadening of NMR lines). Freely speaking, the picture emerging from the present results is that individual atoms are wandering at a rate determined by q^2D_{Li}, q^2D_{Pb}; but the pattern or structure lives longer by the factor $S_{cc}(q)/c_A c_B$.

This comes close to a model of interpenetrating Li and Pb sublattices with rapid exchange *within* sublattices, i.e., to the quasichemical model[37] or to a superionic conductor with two mobile sublattices. The extreme molecular concept—five individual atoms that stick together for a while to form one Li_4Pb molecule—goes beyond the information derivable in the present experiment in two respects, viz., with respect to number and individuality.

C. Continued-fraction representation

The concentration-concentration correlations seen in $S_{cc}(q,E)$ are equilibrium fluctuations of a thermodynamic variable. We have therefore used the continued-fraction formalism[38] which has proven so powerful a description for many linear-response applications. The three-pole form of it with two memory functions does indeed allow very good fits to the data over the full range of q and E (see Figs. 1–4). The same form has served to describe the

molecular-dynamics data for molten NaCl very well.[8] In fact, these data of Adams, McDonald, and Singer[8] are the theoretical result which comes closest to the present experiment, and comparison will be drawn at different places below. The difference between a Mori and a single-Lorentzian description can be seen in Fig. 2 of Soltwisch *et al.*[24]

We start from

$$S_{cc}(q,E)=S_{cc}(q)\frac{\hbar^4\omega_0^2\Omega^2K'/\pi}{(E^2-\hbar^2\omega_0^2+E\hbar^2\Omega^2K'')^2+E^2(\hbar^2\Omega^2K')^2} . \tag{20}$$

The various quantities and their physical implications will be discussed in the following sections.

1. *Moments and characteristic frequency*

The zeroth moment $\langle\omega^0\rangle=S_{cc}(q)$ [Eq. (3)] is not only the full structural information that one can get from the scattering experiment; its importance for the dynamics will also have become apparent by now. It is automatically satisfied by Eq. (20). In Fig. 5 we have compared the integral $\int S_{cc}(q,E)dE$ which has been taken over the limited E range of the present experiment, Eq. (12), with that from a measurement[15] using neutrons of considerably higher energy, $E_0=167$ meV. It is seen that the present results fall, at most, about 5% below those of Ref. 15. If there were strong scattering at energies beyond our range, it would have to show up in this difference. We can thus conclude that there can only be weak scattering intensity outside the quasielastic region for liquid $Li_{0.8}Pb_{0.2}$ at $T=1023-1173$ K.

Knowledge of the zeroth moment fixes also ω_0 which is the second moment divided by the zeroth moment. It is[10(b)]

$$\hbar^2\omega_0^2=\frac{\hbar^2\langle\omega^2\rangle}{\langle\omega^0\rangle}=\frac{1}{S_{cc}(q)}\int E^2S_{cc}(q,E)dE$$
$$=\frac{c_Ac_B}{S_{cc}(q)}\frac{\hbar^2q^2k_BT}{m^*} ,$$

with (21)

$$\frac{1}{m^*}=\frac{c_B}{m_A}+\frac{c_A}{m_B}=\frac{1}{30.83m_a} ,$$

where m_a is the atomic mass unit. With the use of the fit values for $S_{cc}(q)$, $\hbar^2\omega_0^2$ is presented in Fig. 7.

The fourth moment $\langle\omega^4\rangle$ divided by the second moment, $\omega_1^2=\langle\omega^4\rangle/\langle\omega^2\rangle$, determines Ω^2 in Eq. (20),

$$\Omega^2=\langle\omega^4\rangle/\langle\omega^2\rangle-\langle\omega^2\rangle/\langle\omega^0\rangle=\omega_1^2-\omega_0^2 . \tag{22}$$

$\langle\omega^4\rangle$ contains the information about a characteristic frequency of the system, $E_{\rm vib}(q)$, via Eq. (23). $E_{\rm vib}$ can be calculated, in principle, as a sum of integrals containing the interatomic potentials and distribution functions, an explicit expression is given by Abramo, Parinello, Tosi, and Thornton.[39] Then

$$\hbar^4\langle\omega^4\rangle=c_Ac_B\hbar^2\omega_0^2\{3\hbar^2\omega_0^2S_{cc}(q)+[E_{\rm vib}(q)]^2\} . \tag{23}$$

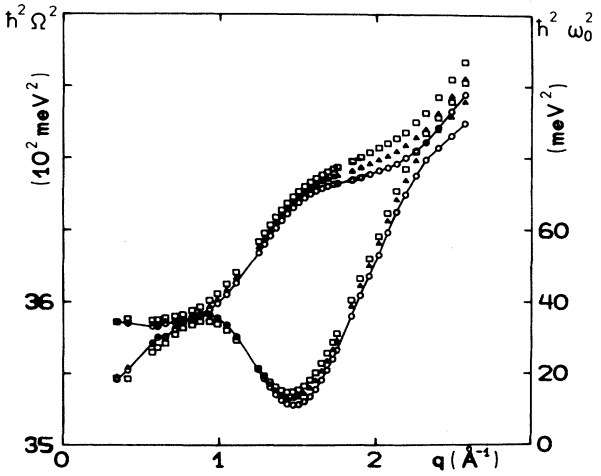

FIG. 7. Moments of the concentration-fluctuation structure factor for liquid Li_4Pb. Circles, triangles, and squares are for 1023, 1098, and 1173 K, respectively. $\hbar^2\omega_0^2$ from Eq. (21) is for lower set of curves and right-hand scale, and uses the fitted $S_{cc}(q)$. Upper set of curves is $\hbar^2\Omega^2$ [Eqs. (22) and (23)] for $E_{\rm vib}=60$ meV and refers to the left-hand scale. In order to help in discerning data sets we have drawn connecting lines between points in Figs. 5–13.

The necessary input information is, however, lacking for the present system.

The characteristic mode(s) of interest here is (are) the longitudinal optical (LO) mode(s), more correctly, the equivalent of the LO mode(s) of a crystal. For binary liquids of type AB the LO mode has been observed in computer simulations, and the situation has been discussed thoroughly, e.g., by Hansen and McDonald for a model of a monovalent molten salt,[6] by Price, Copley, and Rahman for RbBr,[7,40] and by Adams, McDonald, and Singer for NaCl.[8]

There is also extensive analytical work on this subject; see Refs. 41–42(d) and for a review see Ref. 11. But the ratio of atomic masses, the 4:1 stoichiometry, and the presence of conduction electrons make $Li_{0.80}Pb_{0.20}$ different in important respects from the molten salts considered so far in the calculations. The only experimental evidence from a scattering experiment for the LO mode is that Copley and Dolling have found an indication of the expected signal in KBr.[43] Owing to this aspect, the fact that in $Li_{0.80}Pb_{0.20}$ essentially all scattering is found in the quasielastic region as was mentioned above is not too surprising.

At small q, $E_{\rm vib}(q)$ is expected to be of the order of the kinetic ion plasmon frequency $\hbar\omega_{p,\rm ion}$, given by[44]

$$\hbar\omega_{p,\rm ion}=4\pi e^2\left[\frac{Z_A^2}{m_A}\frac{N_A}{V}+\frac{Z_B^2}{m_B}\frac{N_B}{V}\right] , \tag{24}$$

where N_i/V are the number densities. $\hbar\omega_{p,\rm ion}$ amounts to 90 meV for $Z_{\rm Pb}=-4Z_{\rm Li}=-1.6$, and to about 20 meV for $Z_{\rm Pb}=-1.0$. Present estimates for the net ionic charges fall in that range.[16,17] Another "sign" pointing to $E_{\rm vib}$ is that in solid LiI, the LO mode occurs at about 40

meV for $q=0$ (Ref. 45); scaling this value with the melting temperatures, one arrives at 60 meV for Li_4Pb. We do not know how the presence of several optical modes and their coupling to other modes, incomplete ionicity, the presence of electrons, disorder, and high temperature may possibly influence E_{vib}. We have therefore decided to use somewhat arbitrary estimates for $E_{vib}(q)$ in Eq. (23) and to check their influence on the fit parameters. Three different choices were made: two q- and T-independent values of E_{vib}, viz.,

$$E_{vib}(q)=60 \tag{25a}$$

and

$$E_{vib}(q)=40 \tag{25b}$$

(both measured in meV) were chosen, and finally E_{vib} was assigned a weak dispersion which was arbitrarily assumed as

$$E_{vib}(q)=20\ \text{meV}\left[1+\left[\frac{\sin(\pi q/q_0)}{\pi q/q_0}\right]^2\right], \tag{25c}$$

a shape which is in the region of interest similar to that of Bosse and Munakata.[42(a)] The values for Ω resulting from $E_{vib}=60$ meV are presented in Fig. 7. Fit results are presented below for all temperatures using $E_{vib}=60$ meV. The dependence on E_{vib} will be demonstrated by presenting the fit results based on Eqs. (25a)—(25c) for the 1023-K data only, because this set was found to be the most sensitive of the three. Figure 8 shows the systematic trend of χ^2 values for the data measured at 1023 K. The data taken at 1098 and 1173 K behave very similarly, again disfavoring (25c) for $1<q<2$ Å^{-1}.

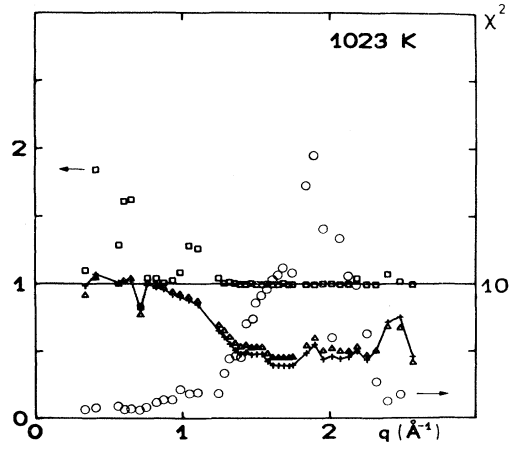

FIG. 8. Fit quality of Mori fits to 1023-K spectra. Values of χ square obtained by using the ansatz $E_{vib}(q)$ of Eq. (25c) are circles (right-hand scale). Normalized to these values and referring to the left-hand scale χ squared for three other choices of parameters are presented: triangles—$E_{vib}=40$ meV, and crosses—$E_{vib}=60$ meV. (We remark here that the higher temperatures give rather similar results.) Included as squares are the results obtained when $E_{vib}(q)$ from Eq. (25c) is used and $\gamma(q)$ is set fixed to 1.2 meV [see Fig. 10(b)].

2. *Memory-function ansatz and fits*

The importance of a good choice for the memory function $K(t)$ is obvious because as a consequence of using the Mori form, most of the detailed information is contained in K, including the coupling of the single variable considered (concentration) to all other degrees of freedom. First, we have tried a single relaxation-time approximation,

$$K(q,t)=\exp[-|t|/\tau_K(q)] .$$

However, definitely unsatisfactory fits were obtained for most of the q range.

The necessity for an ansatz with two relaxation times for the memory function of charge fluctuations had been pointed out by Hansen and McDonald[6] and expounded by Adams, McDonald, and Singer.[8] For diffusion it was used and discussed in Ref. 33. Recently, it was successfully applied to damping of a plasmon mode by Bosse and Munakata.[42(a)] We therefore used the following ansatz:

$$K(q,t)=ae^{-|t|/\tau_2}+(1-a)e^{-|t|/\tau_1} ,$$

whence

$$\begin{aligned} K'(q,E)&=a\frac{\hbar/\tau_2}{E^2+(\hbar/\tau_2)^2}+(1-a)\frac{\hbar/\tau_1}{E^2+(\hbar/\tau_1)^2} , \\ K''(q,E)&=-a\frac{E}{E^2+(\hbar/\tau_2)^2}-(1-a)\frac{E}{E^2+(\hbar/\tau_1)^2} . \end{aligned} \tag{26}$$

The use of Lorentzian shapes for K should be adequate in the quasielastic region. The set of free parameters for each spectrum (q,T fixed) is thus $S_{cc};a;\gamma/2=\hbar/\tau_2;\Gamma/2=\hbar/\tau_1$. Illustratively, the parameters γ and Γ determine the rate at which the otherwise "free" oscillation of concentration fluctuations at the effective frequency Ω is damped.

The fits obtained with this model have been included in Figs. 1—4. Small and large energy regions are displayed separately with better resolution in Figs. 2—4. The agreement reached is considered to be of the order of the systematic experimental errors involved (cf. Sec. IV E), and can be judged from Figs. 1—5 and 8.

In Figs. 9—11 we present the resulting parameter sets a, γ, and Γ. They will be discussed in Secs. V C 3 and V C 4.

It should be noted at the outset that although parameter values are presented for all q, some are of little significance: those at low q ($q\lesssim 0.8$ Å) are very uncertain because there incoherent scattering from ^{7}Li [$I^i(q)$] dominates, and also any value for γ is insignificant if $a\lesssim 10^{-3}$, which occurs in Fig. 9(a) for $T=1173$ K.

3. *Results for the memory function at $E=0$ and connection to diffusional description*

We start again with the elastic scattering, $E=0$, where the combination of parameters

$$\hbar\omega_0^2\tau_{cc}(q)=\hbar^2\Omega^2(q)K'(q,0)=\hbar\Omega^2(q)[a\tau_2+(1-a)\tau_1] \tag{27}$$

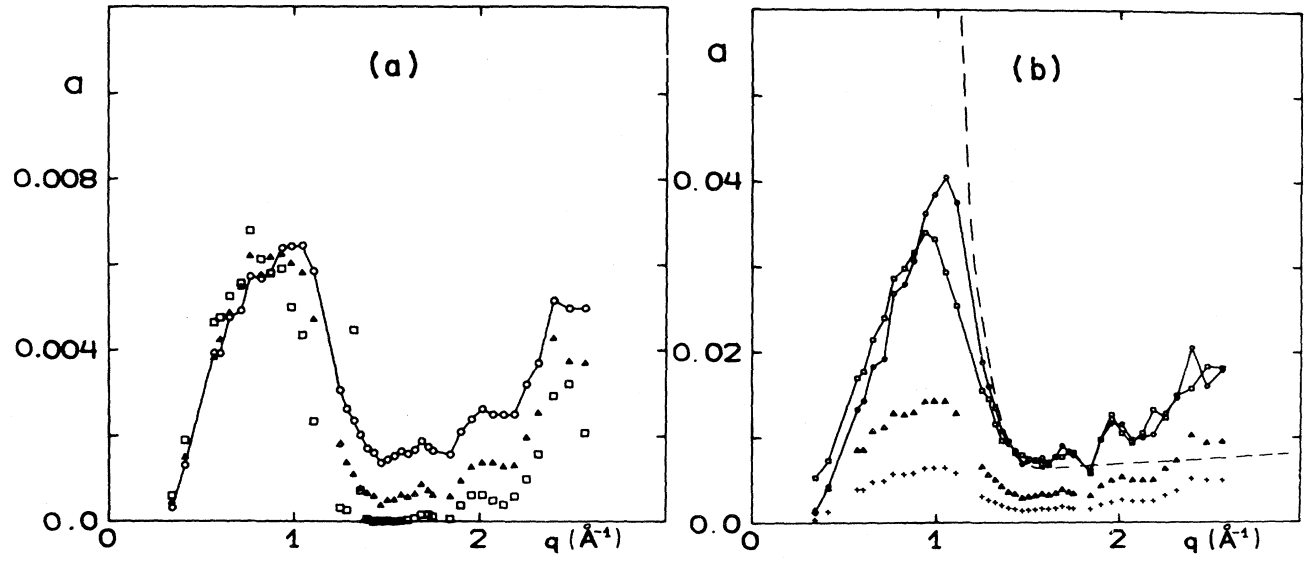

FIG. 9. (a) Intensity of the slow memory channel a of Eq. (26) for liquid Li_4Pb at 1023 K (circles), 1098 K (triangles), and 1173 K (squares); $E_{vib}=60$ meV was used in Figs. 9(a)—13(a). (b) Same for 1023 K and four parameter choices: $E_{vib}=60$ meV (crosses), $E_{vib}=40$ meV (triangles), $E_{vib}(q)$ from Eq. (25c) (circles), and $E_{vib}(q)$ from Eq. (25c), $\gamma(q)=1.2$ meV (squares).

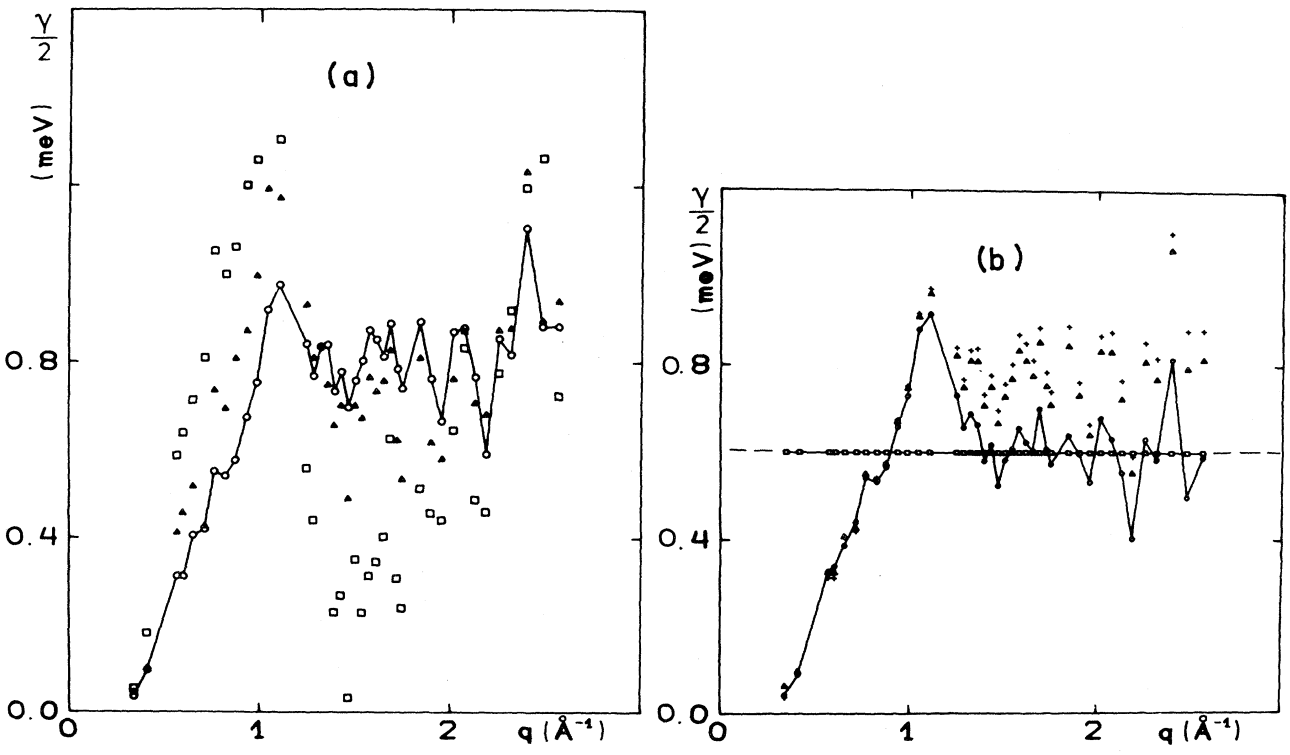

FIG. 10. (a) Width of the slow memory channel $\gamma/2=\hbar/\tau_2$ of Eq. (26) for liquid Li_4Pb. Three temperatures are designated as in Fig. 9(a). Note that 1173-K results (squares) are not significant for $q\approx 1.3$—2 $Å^{-1}$ because there $a\approx 0$ from Fig. 9(a). (b) Same for 1023 K and four parameter choices with values and designations as in Fig. 9(b). $\gamma(q)=$const (squares) was imposed as one choice because this assumption was made in Ref. 8 for the analysis of molten NaCl. Note that this assumption leads to a somewhat lower fit quality (Fig. 8) and a strong rise of $\bar{D}$ [Fig. 12(b)] at low q.

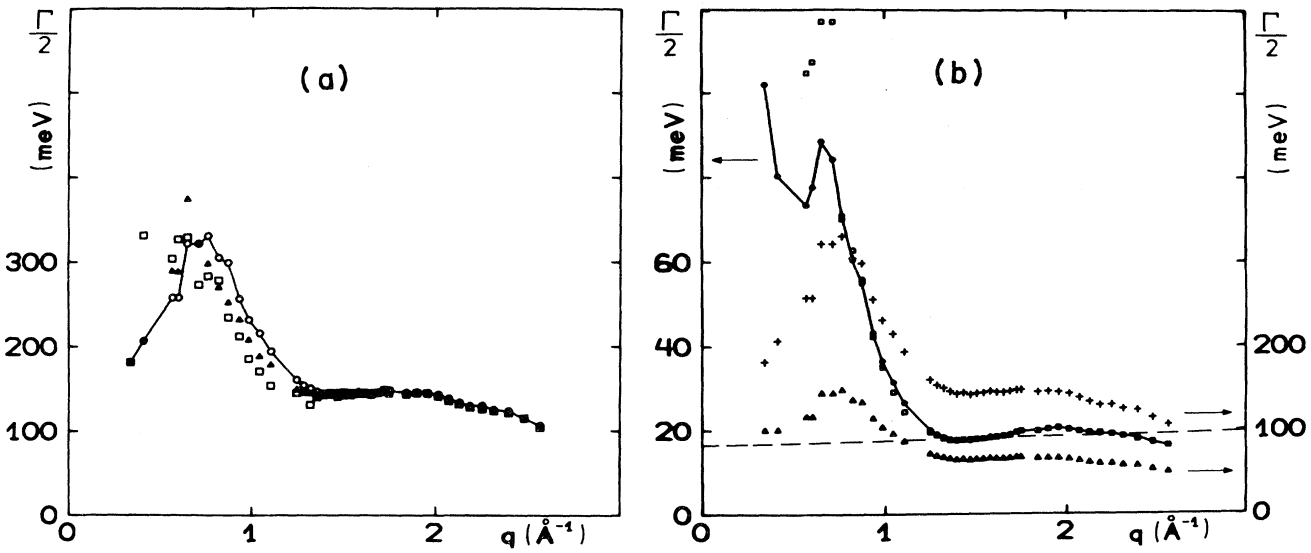

FIG. 11. (a) Width of the fast memory channel $\Gamma/2=\hbar/\tau_1$ of Eq. (26) for liquid Li_4Pb. Three temperatures are designated as in Fig. 9(a). $E_{vib}=60$ meV. (b) Same for 1023 K and four parameter choices with values and designations as in Fig. 9(b). Note the different scales.

is the quantity of importance. Equation (27) shows τ_{cc} of Eq. (18) to be an average of τ_1 and τ_2; this quantity can be taken from Fig. 12 via Eq. (28) for the three temperatures.

We would like to establish here a connection to the diffusion description, and do this by *requiring* agreement between the hydrodynamic [see Eq. (16)] and Mori [Eq. (20)] forms for $S_{cc}(q,E=0)$, whence

$$\bar{D}=\frac{k_BT}{m^*\hbar\Omega^2(q)K'(q,0)}=\frac{k_BT}{m^*}\bar{\tau}(q)\ , \tag{28}$$

in agreement with Eq. (19). The corresponding result has been derived by Sears for density fluctuations by comparing the FWHM of the Mori form (with two time constants in the memory function) with a Lorentzian [see Eq. (34) of Ref. 46]. We present $\bar{D}$ in Fig. 12.

An interesting feature of Fig. 12 is that essentially no trace of the peak structure at q_0 has survived. However, the remaining—though weak—q dependence makes an extrapolation of $\bar{D}$ to $q=0$ less reliable than was thought earlier.[24]

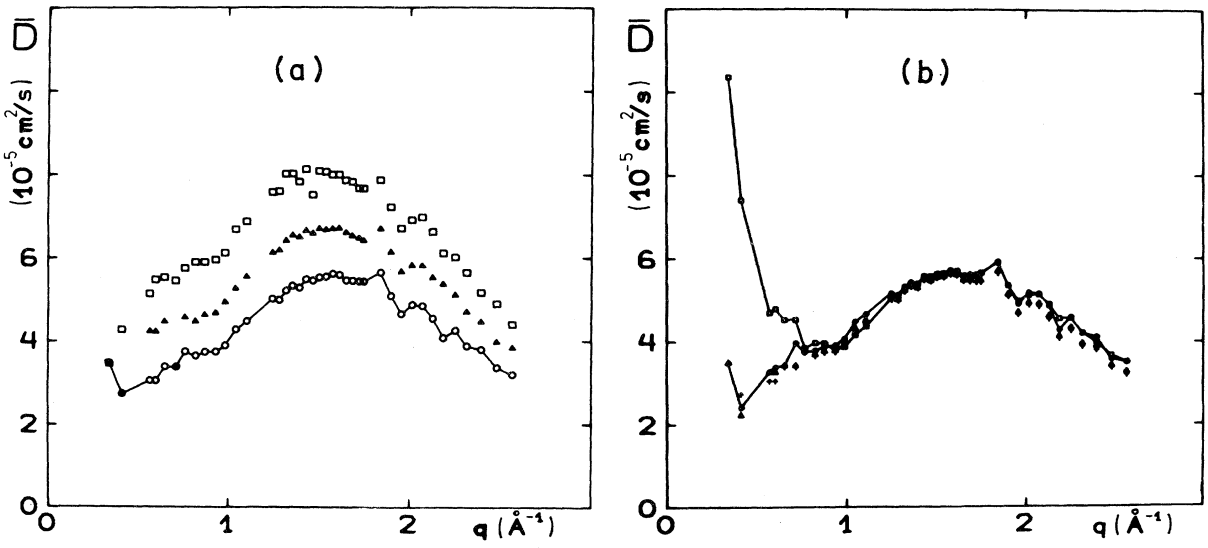

FIG. 12. (a) Diffusion constant $\bar{D}$ of liquid Li_4Pb derived from the Mori fit parameters through Eq. (28). Three temperatures are designated as in Fig. 9(a). Note also that this figure gives essentially the q dependence of $1/K'(q,0)$ because $\Omega^2\approx$const (Fig. 7). (b) Same for 1023 K and four parameter choices with values and designations as in Fig. 9(b).

A pictorial discussion of the relation between effective correlation time (here $\bar{\tau}$) and the underlying dynamical process [here characterized by $\Omega(q)$ and *its* correlation time $K'(q,0)/\hbar$] has been given for an analogous case in orientational diffusion of spins in Ref. 47. When comparing Eq. (28) with the usual expression for diffusion, $D=(k_BT/m)\tau$, one is led to interpret

$$\bar{\tau}(q)=[\hbar\Omega^2(q)K'(q,0)]^{-1}$$

as an effective velocity autocorrelation time of "the average" single particle; see the definition of $\bar{D}$ in Eq. (7b). While τ_{cc} was a "lifetime of agglomerates," $\bar{\tau}$ corresponds then to the effective time constant for diffusion as used, e.g., in Ref. 33, the concept being generalized here to finite q values. This view is corroborated by comparing with the analytical treatment of density fluctuations in a monatomic liquid as developed by Sjögren and Sjölander.[48] In their theory for $S_{NN}(q,E)=S(q,E)$ they point out that the quantity $\pi q^2S(q,0)/S(q)^2$, which in the present case of $S_{cc}(q,E)$ is just $1/(\hbar c_Ac_B\bar{D})\propto[\bar{\tau}(q)]^{-1}$ [Eqs. (16) and (28)], may be described as a sum of two terms: the first derives from self-diffusion of a tagged particle, the second from hydrodynamics of the surrounding. Now in both Ar and Rb, the diffusional term [called $q^2F_s(q,0)$ in Ref. 48], which includes fast, collisional, as well as slow processes in Ref. 48, shows a very weak decrease with q. The corresponding fast and slow channels are here contained in the ansatz for K and in Eq. (27); the weak q dependence can be seen in Fig. 12. On the contrary, the hydrodynamic term shows a strong q dependence in Ref. 48 but there seems to be no correspondence in the present case. The agreement with respect to the diffusional term is thus in accord with the fact mentioned, viz., that $\bar{D}$ is an averaged single-particle diffusion constant.

We compare now with the Mori fit of the molecular-dynamics data of Ref. 8 for molten NaCl; the temperatures are very similar, $1.015T_m$ for NaCl, while 1023 K$=1.04T_m$ for $Li_{0.80}Pb_{0.20}$. The values for $\bar{\tau}(q)$, Eq. (28), of the longitudinal charge-charge correlation were calculated by inserting the parameters α, τ_1, and τ_2 given in Ref. 8 for the present parameters a, $\hbar/\Gamma$, and $\hbar/\gamma$, respectively, and as an approximation ω_{LO} for Ω; the resulting curve for $\bar{D}$ displays an increase by a factor of 10^2 from small q to the position of the structure peak (q_0).

The NaCl data for $\hbar^2\Omega(q)^2K'(q,0)$ thus behave completely differently from the $Li_{0.80}Pb_{0.20}$ data. Actually this is not surprising because the LO mode is well developed in NaCl and its strong dispersion dominates the q dependence of $\bar{\tau}$. Thus the comparison of the scattering at $E=0$ in the present system with monatomic liquids (Ar and Rb, Ref. 48) and with computer simulation of a molten salt (NaCl, Ref. 8) supply indirect evidence that there is no well-developed mode in $Li_{0.80}Pb_{0.20}$.

4. *Results for microscopic parameters of the memory function*

The fit results for the three microscopic parameters determining $K(t)$ are presented in Figs. 9(a), 10(a), and 11(a) where $E_{vib}=60$ meV was used. Their dependence on E_{vib} is shown in Figs. 9(b), 10(b), and 11(b) for the 1023-K data. In Figs. 9(b)—11(b) the corresponding results for molten NaCl from Ref. 8 have been included, scaled at $q=1.25$ Å^{-1} to the fit results which are based on Eq. (25c).

In Figs. 9(a)—11(a) one notes the strong temperature dependence of the parameter a of the slow part of K, and a weak temperature dependence of the fast part, $1-a$ and Γ. The strong temperature dependence of $\bar{D}$ and $\bar{\tau}$ [see Fig. 12(a)] is thus due to a rapid buildup of the slow process as T is lowered toward T_m. We mention here that the diffusion constants (D_{Li}, $\bar{D}$, and also D^+; see Table II) have apparent activation energies E_A in the range of 6—8 kcal/mol (where the uncertainty of E is of the order of the differences between the three values). That these values are in accord with the "rule of thumb"[49] $E_A\simeq 3.7k_BT_m$ may be useful for applications of the present findings to other heterocoordinated alloys.

From Figs. 9(b)—12(b) we may note that the characteristic q dependence of a, γ, Γ, and $\bar{D}$ apparently does not depend critically on the value assumed for E_{vib} as long as the dispersion is reasonably small (although the numerical values of a and Γ do). This is mainly due to the fact that Ω is very likely larger than the E range covered by the experiment (see the end of Sec. V C 1).

Comparisons with the NaCl parameters of Ref. 8, the dashed lines in Figs. 9(b)—11(b), can only be drawn with strong mental reservations because of the qualitative difference between the systems. When it is nevertheless done, one notes agreement in some respects: order-of-magnitude ratio between γ and Γ, $a\ll 1$ [these two statements apply also to the fast and slow memory functions in molten LiBr (Ref. 33)], sharp kink of a below q_0, and weak q dependence of γ and also of Γ if $q\gtrsim 1$ Å^{-1}. But there is at least as much disagreement, even qualitative: indication for saturation of a at $q<1$ Å^{-1}, and rise of Γ below 1 Å^{-1}. Both these features appear to be essentially independent of the choice of E_{vib}. The slow time constant $1/\gamma$ is essentially q independent for 1023 K as is τ_2 in NaCl.

When one tries to analyze the agreements or discrepancies, one must try to understand the physical mechanisms behind the slow and fast memory part. At the present stage, we can only offer some speculations.

It appears plausible to us that the fast part Γ in the form found for NaCl and for Li_4Pb at larger q ($q\gtrsim q_0$), i.e., q independent, should be ascribed to the near-field interactions, in particular to collisions. There is an obvious discrepancy between NaCl and Li_4Pb in the fast memory channel for smaller q,Γ ($q<1$ Å^{-1}). We would like to speculate here that the increase of Γ is due to an additional process and that its explanation may lie in the fact that Γ increases in the q range below the inverse effective shielding length λ of the conduction electrons which has been derived by Evans *et al.* from $S_{cc}(q)$ as $\lambda\simeq 1$ Å.[16] The increase of Γ for $q<1$ Å^{-1} may then be due to the possibility of relaxation of the characteristic concentration-fluctuation excitation, by energy transfer to conduction electrons (which are in turn coupled to other degrees of freedom), i.e., due to the fluctuation aspect of Joule heating, observed on the ions. The hypothesis is checked qualitatively in the Appendix by deriving from

the known electrical resistivity[50] an order-of-magnitude estimate of the rate of perturbation of ionic motion. A possible contribution to Γ of the order of 0.1 eV is obtained. More precise measurements will be necessary to resolve this question, mainly because incoherent scattering from Li is by no means negligible in this q range (see Fig. 3).

As to the parameter a which determines the importance of the slow part of the memory function, it may be helpful to remember that in the Mori description of $S(q,E)$ of monatomic liquids a is determined by the ratio c_p/c_v (see, e.g., Refs. 46 and 51), i.e., by the stability against isothermal and adiabatic density fluctuations, because $c_p/c_v=(\partial V/\partial p)_T/(\partial V/\partial p)_S$. A similar relation might be expected to apply to $S_{cc}(q,E)$ since $S_{cc}(q)$ corresponds to the stability against concentration fluctuations [Eq. (4)]. The combination of parameters of the Mori description which equals c_p/c_v-1 in a monatomic liquid may be evaluated for the present case, where it is

$$a'=\frac{a}{\omega_0^2/\Omega^2}=\frac{a}{\hbar\tau_{cc}^{-1}/[K'(q,0)]^{-1}} . \tag{29}$$

Numerically, one obtains values of the order $0.5,\ldots,1$ (depending on E_{vib} and T) (see Fig. 13). The value for NaCl (Ref. 8) is 0.02 at the structure peak, and in liquid Ar it was 1.2, independent of q.[46] A possible qualitative conclusion from this observation, a not small compared to 1, is that excitation of the two independent variables thermodynamically determining the concentration c (T and μ) are strongly coupled.

VI. SUMMARIZING REMARKS

The present study is, to our knowledge, the first scattering experiment on the microscopic dynamics of heterocoordination in a binary real liquid. For experimental reasons we have chosen $^7Li_{0.8}Pb_{0.2}$, a liquid which is more complicated than the binary liquids studied so far in theoretical or computer-simulation work; we had also to restrict the energy and q range covered.

Quasielastic scattering from liquid $Li_{0.80}Pb_{0.20}$ exhibits a strongly peaked structure centered at $q=1.5$ Å^{-1}, $E=0$, due to its now well-known strong CSRO. A diffusional interpretation of the data yields the interdiffusion constant D^+ at finite q which can be related in a simple, approximate way to the self-diffusion constants and the structure [Eq. (15)]. It also allows a rather precise description of the zero-frequency spectral density $S_{cc}(q,E=0)$, which in the present system almost diverges around $q=1.5$ Å^{-1} as $T\rightarrow T_m$. We have also compared the concentration-fluctuation picture with the concept of formation of "molecules" or "aggregates" and derived estimates of the corresponding lifetime (see Fig. 6).

Application of these concepts to other liquids with compound-forming tendency requires either $S_{cc}(q)$ plus the self-diffusion constants, or more realistically, thermodynamic data and a model for the short-range order expected (both often exist), plus data or estimates for the self-diffusion constants of the constituents; information on the latter seems to be rare.

An interpretation which is more satisfactory from the formal point of view is the third-step Mori description. As a key input it requires the eigenfrequency (versus q) of the variable considered, E_{vib} in Eq. (23). No evidence for an underdamped optical mode could be seen in the present experimental data, nor was clear evidence for it found in the analysis; however, the fits suggest $E_{\text{vib}}>20$ meV. Yet the spectral shape might be somewhat less smooth than what has so far been apparent from fitting the Mori expression Eq. (20). This is suggested by a slight but seem-

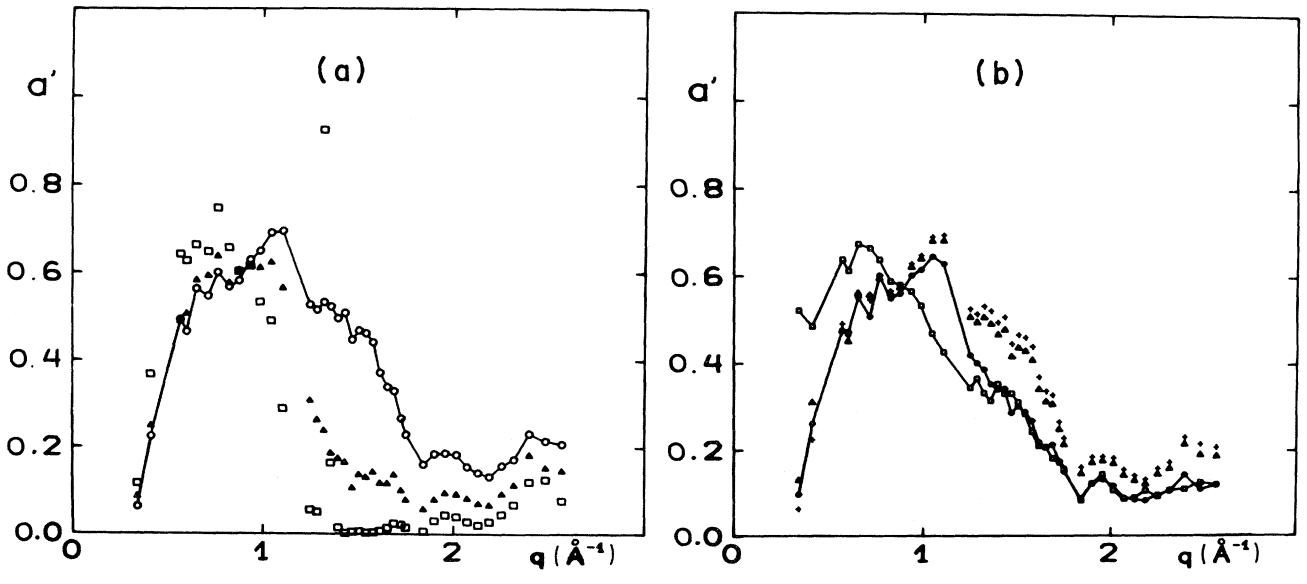

FIG. 13. (a) Coupling parameter $a'=a\Omega^2/\omega_0^2$ introduced in Eq. (29) for liquid Li_4Pb. Three temperatures are designated as in Fig. 9(a). (b) Same for 1023 K and four parameter choices with values and designations as in Fig. 9(b).

ingly systematic modulation of the data around the "best-fit curves." We present a plot which emphasizes this fact in Fig. 4, not without repeating that the magnitude of the deviations noticeable at $E \gtrsim 3$ meV is of the order of the systematic uncertainties of the present experiment which was aiming mainly at the quasielastic region.

Concerning the microscopic parameters derived there is independence of the major uncertainty (namely the value of $E_{\rm vib}$) in the values and q dependence for γ, $\bar{D}$, and a', and essential independence of the shape versus q for a and Γ. For the memory function $K(q,t)$ a sum of two exponentials has been successful. The shape of $K(q,E=0)$ suggests that it is dominated by single-particle diffusion. K achieves an essentially complete overdamping of the characteristic (i.e., LO) mode.

This may be compared with analytic calculations for molten salts by Gaskell.[52] As to the details of $K(q,E)$, several gross features are similar to those found for liquid NaCl,[8] notably the relative importance and relative time scale of a "slow" and "fast" channel. There appears to be one contribution to the *fast* channel which is active only for $q < 1$ Å^{-1} (Fig. 11); it may be the dynamic signature of the presence of conduction electrons in liquid Li_4Pb.

From the comparison with the NaCl results[8] we conclude that some effects play less of an explicit role than might have been anticipated: the large mass ratio and the large number ratio, or the polarizabilities which we would expect to be large in the present system. However, it might be their combined action which is responsible for the overdamping of the LO mode. The fact that polarizability of the ions leads to considerable changes of the dynamic properties of a molten salt has been demonstrated clearly in computer-simulation work.[53] Finally, it may be stressed again that the temperature dependence of the quasielastic (and in particular the $E=0$) spectrum is very strong; this temperature dependence is essentially due to the *slow* memory channel.

ACKNOWLEDGMENTS

This work was supported in part by Deutsche Forschungsgemeinschaft through Sonderforschungsbereich 161. We are obliged to the Fritz-Haber-Institut, Berlin, for computer time.

APPENDIX

The influence which the scattering of conduction electrons from concentration fluctuations has on the dynamics of the concentration fluctuations themselves is in a way the inverse of Baym's problem.[54] It will be considered here in a very rough estimate, using nearly-free-electron (NFE) approximations throughout. The experimental value for the electrical resistivity is $\rho = 1/\sigma = 5 \times 10^{-4}$ Ω cm.[50,55] Conduction is essentially all electronic (from the order of magnitude) and determined by scattering of electrons off concentration fluctuations (from comparison with $\rho_{\rm Li}$ or $\rho_{\rm Pb}$). In $1/\rho = (N_e/V)(e^2/m)\tau_e$ we estimate the electron density N_e/V in two ways. (a) The screening length $1/\lambda \approx 1$ Å^{-1} from[16] points to about 2 free electrons per formula unit Li_4Pb or $k_F \simeq 0.85$ Å^{-1}. This is derived from $\lambda^{-2} = 2me^2 k_F/\pi\hbar^2$ with $k_F = (3\pi^2 N_e/V)^{1/3}$. The density reduction of 20% (Ref. 56) was taken into account. (b) Following the suggestion of Nagel and Tauc[57] that the structure factor S_{cc} is the main determinant for ordering energy, one may expect $2k_F$ to coincide with q_0 (neglecting ionic contribution to the bonding though); thus $k_F = 0.75$ Å or 1.3 electrons per formula unit. With the use of 1.4 electrons per Li_4Pb, the NFE ansatz yields (in s)

$$\tau_e = 0.56 \times 10^{-15} ,$$

corresponding to a mean free path of 9 Å or two times $2\pi/q_0$.

The number of collisions which each formula unit undergoes per time follows from $N_e/\tau_e = N_f/\tau_f$, with N_f/V as the number of formula units per volume, as $1/\tau_f = 2.5 \times 10^{15}$ s^{-1}. [As to the meaning of τ_f, $1/\tau_f$ is *part* of the rate $1/\tau_1$ introduced by Eq. (26).]

The number of collisions needed to relax the characteristic excitation can be estimated from the momentum or energy change imparted on the lighter atom, Li, by the electrons. The relative momentum change per collision is $\simeq 2\hbar k_F/p_{\rm Li} = 0.08$, while the energy change is $2\hbar k_F v_{\rm Li}/E_{\rm Li} = 0.34$, both from $E_{\rm Li} \simeq k_B T$ and the prevalence of large-angle scattering events for ρ. Energy relaxation is thus expected to occur faster than momentum relaxation, roughly after $(1/0.34)^2 = 10$ collisions due to the random nature of the collisions. That leads then to a damping rate of 0.25×10^{15} s^{-1} or $\Gamma = 165$ meV. With the rough assumptions used, this can of course be an order-of-magnitude estimate only. For $q \to 0$, the process considered is presumably connected to the additional Lorentzian caused by (electronic) heat conduction [see remark after Eq. 6(b)].

---

*Permanent address: Institute für Angewandte Kernphysik I, Kernforschungszentrum Karlsruhe, Postfach 3640, D-7500 Karlsruhe, Germany.

[1]K. L. Komarek, Ber. Bunsenges. Phys. Chem. 80, 936 (1977); B. Predel, *ibid.* 80, 695 (1976).

[2]A. Boos, P. Lamparter, and S. Steeb, Z. Naturforsch. 32A, 1222 (1977).

[3]P. Chieux and H. Ruppersberg, J. Phys. (Paris) Colloq. 41, C8-145 (1980).

[4]M. von Hartrott, J. Höhne, D. Quitmann, J. Rossbach, E. Weihreter, and F. Willeke, Phys. Rev. B 19, 3449 (1979).

[5]S. W. Haan, R. D. Mountain, C. S. Hsu, and A. Rahman, Phys. Rev. A 22, 767 (1980).

[6]J. P. Hansen and I. R. McDonald, Phys. Rev. A 11, 2111 (1975).

[7]J. R. D. Copley and A. Rahman, Phys. Rev. A 13, 2276 (1976).

[8]E. M. Adams, I. R. McDonald, and K. Singer, Proc. R. Soc. London Ser. A 357, 37 (1977).
[9]G. Ciccoti, G. Jaccucci, and I. R. McDonald, Phys. Rev. A 13, 426 (1976).
[10](a) C. Cohen, J. W. H. Sutherland, and J. M. Deutsch, Phys. Chem. Liq. 2, 213 (1971); (b) A. B. Bhatia, D. E. Thornton, and N. H. March, *ibid.* 4, 97 (1974).
[11]M. Parinello and M. P. Tosi, Rev. Nuovo Cimento 2, 6-1 (1979).
[12]M. Baus and J. P. Hansen, Phys. Rep. 59, 1 (1980).
[13]A. Zulkin and W. R. Ramsey, J. Phys. Chem. 62, 689 (1958).
[14]H. Ruppersberg and H. Egger, J. Chem. Phys. 63, 4095 (1975).
[15]H. Ruppersberg and H. Reiter, J. Phys. F 12, 1311 (1982).
[16]A. P. Copestake, R. Evans, W. Schirmacher, and H. Ruppersberg, J. Phys. C (in press).
[17]C. Holzhey, F. Brouers, J. R. Franz, and W. Schirmacher, J. Phys. F 12, 2611 (1982).
[18]A. B. Bhatia and R. N. Singh, Phys. Lett. 78A, 460 (1980).
[19]K. Hoshino and W. H. Young, J. Phys. F 10, 1193 (1980); 10, 1365 (1980).
[20]A. B. Bhatia and D. E. Thornton, Phys. Rev. B 2, 3004 (1970).
[21]B. Mozer, D. L. Price, D. T. Keating, and H. Meister, Phys. Lett. 30A, 206 (1969).
[22]M. Soltwisch, D. Quitmann, H. Ruppersberg, and J.-B. Suck, J. Phys. (Paris) Colloq. 41, C8-167 (1980).
[23]M. Soltwisch, D. Quitmann, H. Ruppersberg, and J.-B. Suck, Phys. Lett. 86A, 241 (1981).
[24]M. Soltwisch, D. Quitmann, H. Ruppersberg, and J.-B. Suck, in *Ionic Liquids and Polyelectrolytes,* Vol. 172 of *Lecture Notes in Physics,* edited by K. H. Bennemann, F. Brouers, and D. Quitmann (Springer, New York, 1982), p. 136.
[25]N. H. March and M. P. Tosi, *Atomic Dynamics in Liquids* (MacMillan, London, 1976), Chap. 6.
[26]L. S. Darken, Trans. AIME 175, 184 (1948).
[27]W. Becker, thesis, Universität Saarbrücken, 1979 (unpublished).
[28]I. A. Blech and B. L. Averbach, Phys. Rev. 137, 1114 (1965).
[29]J. R. D. Copley, Comput. Phys. Commun. 9, 59 (1975).
[30]J. S. Murday and R. M. Cotts, Z. Naturforsch. 20A, 85 (1974); A. Ott and A. Lodding, *ibid.* 26A, 1578 (1965).
[31]K. Sköld, Phys. Rev. Lett. 19, 1023 (1967); see also K. Sköld, J. M. Rowe, G. Osbrowkoski, and P. D. Randolph, Phys. Rev. A 6, 1107 (1972).
[32]G. Doege, Z. Naturforsch. 20A, 634 (1965).
[33]F. Lantelme, P. Turq, and P. Schofield, J. Chem. Phys. 71, 2507 (1979).
[34]M. W. Johnson, N. H. March, D. I. Page, M. Parinello, and M. P. Tosi, J. Phys. C 8, 751 (1975); B. Predel and G. Oehme, Z. Metallkd. 70, 450 (1979).
[35]A. B. Bhatia and V. K. Ratti, J. Phys. F 6, 927 (1976).
[36]If one were to formulate the claim "there are long-lived agglomerates" by saying "there is a certain fraction of agglomerates on the average, *and* these are long lived," then one comes back to $S_{cc}(q,0)$, the maximum value of which peaks out by an order of magnitude in Fig. 6.
[37]E. A. Guggenheim, *Mixtures* (Clarendon, Oxford, 1952).
[38]H. Mori, Prog. Theor. Phys. 34, 399 (1965).
[39]M. C. Abramo, M. Parinello, M. P. Tosi, and D. E. Thornton, Phys. Lett. 43A, 483 (1973).
[40]D. L. Price and J. R. D. Copley, Phys. Rev. A 11, 2124 (1975).
[41]L. Sjögren and F. Yoshida (private communication).
[42](a) J. Bosse and T. Munakata, Phys. Rev. A 24, 2261 (1981); 25, 2763 (1982); (b) D. K. Chaturvedi, U. Marini Bettolo Marconi, and M. P. Tosi, Nuovo Cimento 57, 319 (1980); (c) P. K. Kahol, O. K. Chaturvedi, and K. N. Pathak, J. Phys. C 11, 4135 (1978); (d) T. Gaskell and M. S. Woolfson, *ibid.* 15, 6339 (1982).
[43](a) J. R. D. Copley and G. Dolling, J. Phys. C 11, 1259 (1978); (b) F. Yoshida, *ibid.* 14, 573 (1971).
[44]J. P. Hansen, I. R. McDonald, and P. Vieillefosse, Phys. Rev. A 20, 2590 (1979).
[45]H. Bilz and W. Kress, *Phonon Dispersion Relations in Insulators,* Vol. 10 of *Springer Series in Solid State Sciences* (Springer, New York, 1979), pp. 32 and 33.
[46]V. F. Sears, Can. J. Phys. 48, 616 (1969).
[47]D. Quitmann, in *Site Characterization and Aggregation of Implanted Atoms in Materials,* edited by A. Perez and R. Coussement (Plenum, New York, 1980), p. 139.
[48]L. Sjögren and A. Sjölander, Ann. Phys. (N.Y.) 110, 421 (1976); 110, 156 (1976); see also J. Phys. C 12, 4369 (1979).
[49]F. D. Richardson, *Physical Chemistry of Melts in Metallurgy* (Academic, London, 1974), p. 8.
[50]V. T. Nguyen and J. E. Enderby, Philos. Mag. 35, 1013 (1977).
[51]C. H. Chung and S. Yip, Phys. Rev. 182, 323 (1969).
[52]T. Gaskell, J. Phys. C 15, 1601 (1982).
[53]M. Dixon and M. J. L. Sangster, J. Phys. C 9, 909 (1976); J. Jaccucci, I. R. McDonald, and A. Rahman, Phys. Rev. A 13, 1581 (1976).
[54]G. Baym, Phys. Rev. 135, A1691 (1964).
[55]C. van Marel, W. Geerstma, and W. van der Lugt, J. Phys. F 10, 2307 (1980).
[56]H. Ruppersberg and W. Speicher, Z. Naturforsch. 31A, 47 (1970).
[57]S. R. Nagel and J. Tauc, Phys. Rev. Lett. 35, 380 (1975).